



Study of Thermal Behavior and Anti-Breast Cancer Activity of Some New Lignin-Nanoparticle Networks Sustained with Triterpenoid Compound Isolated from *Calotropis procera* L. leaves



Enass A. Zghair Al-Suwaytee, Baqer A. Al-Mayyahi*, Adnan J.M. Al-Fartosy
Department of Chemistry, College of Science, University of Basrah, Basrah, Iraq.

THE AIM of the present study is to provide breast cancer antibiotic from compound extracted from a cheap and available local plant (*Calotropis procera* L.) and preparation new two interpenetrating polymer networks (IPNs) based on biopolymer product, nature (lignin nanoparticles LNPs) and manufactured as methacrylic acid (MAA) and 2-(Dimethylamino)ethyl methacrylate (DMAEMA) were identified and evaluated by IR, thermal analysis (TGA) and scanning electron microscopy (SEM) to carry the plant extract. The efficacy of all plant extract, LNPs, and IPNs for the extract was tested using 3-(4,5-dimethylthiazol-2-yl)-2,5-diphenyltetrazolium bromide (MTT assay) on the MCF-7 cell line for 72 h and different concentrations. We found that all models gave different lethal effect to the cells.

Keywords: Lignin, Lignin-Nanoparticles, Anti-Breast Cancer, IPNs, *Calotropis procera* L.

Introduction

The term "biopolymers" is commonly used to describe polymers produced from living species in a natural way. Their molecular backbones are made out of repeating units of saccharides, nucleic acids, or amino acids and sometimes various additional chemical side chains contributing also to their functionalities. In spite of the bigger part of biopolymers is extracted from biomass, such as polysaccharides from cellulose and proteins from collagen or milk, biopolymers can also be produced from bio-monomers using conventional chemical processes as polylactic acid, or straightforwardly in microorganisms or hereditarily modified living beings [1, 2]. Biopolymers are generally divided into two broad, bio-degradable and non-biodegradable [3]. Biodegradable polymers define as polymers that are degradable in vivo, this can be done either enzymatically or non-enzymatically, to produce biocompatible or nontoxic by-products [3]. They can keep their mechanical quality and other material execution attributes amid functional application, yet that is at last corrupted to low sub-atomic weight mixes, for example, H₂O, CO₂ and other

non-lethal results [4]. Biodegradation happens just inside the biosphere as microorganisms assume a focal job in the biodegradation procedure. Biodegradation happens through the action of enzymes and/or chemical deterioration associated with living organisms. This occasionally happens in two stages. The first is the shatter of the polymers into short length of chains by methods for either abiotic responses, i.e. oxidation, photo degradation or hydrolysis, or biotic responses, i.e. corruptions by microorganisms. This is trailed by bio-assimilation of the polymer parts by microorganisms and their mineralization [4]. They are eminent on traditional non-degradable polymers because they remain in bodies after being implanted and do not need subsequent surgery to remove them. Thus, they have gained widespread application in the biomedical domain in recent years, such as tissue engineering, gene delivery, drug delivery, and bio-imaging [5-7]. For example:

Lignin

It is the only aromatic polymer found in wood. The amount of lignin in ordinary wood is 20% -35% depending on different types of wood and

*Corresponding author e-mail: baqer.almayyahi@yahoo.com

Received 13/12/2018; Accepted 16/1/2019

DOI: 10.21608/ejchem.2018.6617.1555

©2019 National Information and Documentation Center (NIDOC)

is mainly concentrated in the middle plate area where Lignin is associated with cellulose and hemicelluloses[8]. Lignin has a large potential as a big-volume feedstock to produce high-quality products, as resistance to decay and biological attacks, high stiffness, UV absorbance, and anti-oxidant[9]. The main drawbacks to the use of lignin in many applications are that it is not homogeneous/morphological and low solubility in water, so when converted into nanoparticles merged form and size, increases its solubility and expands its use in different applications[10]. Polymeric nanoparticles have been considered as the most productive vehicles for drug conveyance due to their great pharmacokinetic properties[11]. Nanoparticles (NPs) are alluring for therapeutic reasons for existing depends on their essential and interesting highlights, for example, their surface to the mass proportion that is significantly bigger than that of different particles, their quantum properties and their capacity to adsorb and convey different compounds. NPs have a moderately large (functional) surface which can tie, adsorb and carry other compounds, for example, drugs, probes, and proteins[12]. The field of nanoparticle drug delivery supply a further chance for the improved oncology, meanwhile the delivery of both old and new chemotherapy[13], either source non-biodegradable polymers bio-based and being non-biodegradable[14].

Poly (N, N-dimethyl amino ethyl methacrylate) (PDMAEMA) as an example, it is major used polymer. It joins its frail polyelectrolyte conduct with thermo sensitivity[15]. Subordinate on the

pH, the polymer moves toward becoming water-insoluble, over a specific temperature attributable to a lower critical solution temperature [16-18].

Study Plant:

Distribution and Common names of Calotropis procera

Calotropis procera (Fig. 1) is a plant widely distributed in Asia, Africa, and America. It is native to West Africa as far south as Angola,

Kingdom: Plantae

Order: Gentianales

Family: Asclepiadaceae (Milkweed family)

Genus: *Calotropis*

Species: *Procera*

North and East Africa, Madagascar, India, Pakistan, Nepal, Afghanistan, Algeria, Iran, Iraq, Palestine, Kuwait, Oman, Saudi Arabia, United Arab Emirates, Yemen, Vietnam, Niger, Nigeria, Kenya, Zimbabwe, southern Asia, and Indochina to Malaysia. The species is now naturalized in Australia, many Pacific islands, Mexico, Central and South America, and the Caribbean islands[19, 20]. Common names for the plant include the following: Arabic: dead sea plant, debaj, usher, oshar, kisher; English: calotrope, calotropis, dead sea fruit, desert wick, giant milkweed, swallow-wort, mudar fiber, rubber bush, rubber tree, sodom apple.

Description and Taxonomic classification

It is a soft-wooded, evergreen, perennial shrub. It has one or a few stems, few branches, and



Fig. 1. *Calotropis procera*

relatively few leaves, mostly concentrated near the growing tip. The bark is corky, furrowed, and light gray. A copious white sap flows whenever stems or leaves are cut. Giant milkweed has a very deep, stout taproot with few or no near-surface lateral roots. Giant milkweed roots were found to have few branches and reach depths of 1.7 to 3.0 m in Indian sandy desert soils. The opposite leaves are oblong-obovate to nearly orbicular, short-pointed to blunt at the apex and have very short petioles below a nearly clasping heart-shaped base. The leaf blades are light to dark green with nearly white veins. They are 7 to 18 cm long and 5 to 13 cm broad, slightly leathery, and have a fine coat of soft hairs that rub off. The flower clusters are umbelliform cymes that grow at or near the ends of twigs. The flowers are shallowly campanulas with five sepals that are 4 to 5 mm long, fleshy and variable in color from white to pink, often spotted or tinged with purple. The fruits are inflated, obliquely ovoid follicles that split and invert when mature to release flat, brown seeds with a tuft of white hairs at one end [21, 22].

This study embarked on to explore the following aims:

To isolate and identify of some chemical active compounds from leaves of Iraqi *Calotropis Procera* L. plant. To synthesis of some new drug delivery IPNs as a novel lignin nanoparticles loaded with the isolated active compound from *Calotropis procera* L. Carry out thermal analysis study to assess the mechanical characteristic of the synthetic nanoparticles. Besides, to study the in vitro cytotoxicity on MCF-7 human breast cancer cell line by using MTT [(3-(4, 5-dimethyl thiazol-2-yl)-2, 5- diphenyl tetrazolium bromide, a tetrazol] assay.

Experimental

Materials

All chemicals used in this study were of analytical grade, N,N-dimethylamine ethyl methacrylate (fresh distilled), Dimethyl formaldehyde (Assay $\geq 99.8\%$), Potassium hydroxide, N, N- Methylene bis-acrylamide and Meth acrylic acid (fresh distilled) (Assay $\geq 99\%$) were purchased from (Sigma Aldrich). Absolute Acetone, Absolute Ethanol from (VWR). Absolute Methanol, Diethyl ether (Assay $\geq 99\%$) from (SCH). ethylene glycol (Assay $\geq 98\%$), dichloromethane (DCM), and chloroform (Assay $\geq 99.5\%$) were

supplied by MACRON Company, petroleum ether (Assay ≥ 99.9) from (SCHARLAU), sulfuric acid (Assay $\geq 96\%$) from (Fluka). Silica gel from (HIMEDIA). Trypsin/EDTA, Fetal bovine serum, RPMI 1640 were supplied by (Capricorn) Germany Company.

Petroleum ether extract of Calotropis procera L. leaves

100 gm of *Calotropis procera* L. leaves were continuously extracted by soxhlet in the form meals using 2000 ml of petroleum ether (40-60 °C) for (12 h) and the solvent removed under reduced pressure in a rotary evaporator to afford (2.5595 gm) of oil [23].

Separation and Identification of Phytoconstituents from Petroleum Ether extract of Calotropis procera L. leaves

Saponification of Petroleum Ether-Extracts

5 gm of petroleum ether extract of *Calotropis procera* L. leaves was refluxed with 2 gm of KOH in 40 ml ethanol for 1 hour. Then, it was transferred into separating funnel with the help of 100 ml boiling water, cool it slightly and while warm and shaken with solvent ether (3×100 ml). Various ether portion was combined in separating funnel and extracted with water (3×40 ml) and 3% solution of KOH (3×40 ml) and then washing with 40 ml water till the alkali get neutralized. The solvent ether extracts concentrate and dried [24].

Separation of Phytoconstituents from Unsaponifiable Matter of Calotropis procera L. leaves by Column Chromatography

Column chromatography was performed to separate of Phytoconstituents from an unsaponifiable matter of *Calotropis procera* L. leaves. A glass column size (2.5×60 cm) was plug down to the bottom with small glass wool, and then packed with silica-gel (mesh 60-120 μm). The slurry was prepared by dissolving 50.5g of silica-gel in 200 ml of CHCl₃: Methanol (9.5:0.5) as eluent. The solid residue was then loaded to the top of the column and fractions of 5 ml were collected and monitored by TLC. Fractions were collected and dried at room temperature [25, 26].

Preparation of Rice husks and lignin extraction

Extraction, isolation and purification of lignin

The husks of Iraqi Rice (*Oryza Sativa* L. from Poaceae family) were obtained on September 2017 from the local farms in the district of Kufa (Province of Najaf), Iraq. It was dried in an oven at 60 °C for a period of 5 h to removed moisture,

then grind and kept the powder in plastic containers at room temperature until time of use. A quantity (100 g) of powdered rice husks were extracted in a Soxhlet apparatus with petroleum ether (40-60 °C) - ethanol (2:1), for 24 h to remove the extractives (proteins, wax, and lipids) of cells wall. The residue was dryness to afford 99.67 g of dry extract. Then, the residue was extracted in a Soxhlet apparatus with ethanol-water (7:3), for 24 h using sulfuric acid (in proportions 3.0% v/v) as a catalyst. The extract was filtrated, and the obtained filtered is evaporated in a rotary evaporator and added to 500 ml of cold water to precipitation lignin. Finally, the lignin is washed, dried to afford 7.7158g and kept at room temperature until time of use[27], as shown in Fig. 2.

Preparation of Lignin Nanoparticles (LNPs)

1.4 g of lignin dissolved in 250 ml ethylene glycol, under stirring for 6 h at room temperature prior to filtration through a 0.4 mm micro filter paper in order to remove the insoluble impurities from lignin. Hydrochloric acid (8.00 ml) was add to 90 ml of the filtered lignin solution at a rate of 0.5 ml/min, the solution was then dialyzed in a 1L bottle for three days changing the water two

times daily. The resulting product was recovered by precipitation (at pH=2) with a 1N HCl solution and then separated by stagnating. The solid phase was washed twice with distilled water and subsequently dried and weighed [28].

Preparation of interpenetrating polymer networks (IPNs)

Preparation of PDMAEMA-LNPs IPN

1g of DMAEMA (distilled fresh) and 0.5g of LNPs dissolved in 10ml DMF. The cross-linked agent (N, N-methylene bisacrylamide) 10% and trace amount from initiator was add. The mixture placed under a nitrogen atmosphere for half hour to expel dissolved oxygen and placed in UV Irradiation Device (365nm) for Photopolymerization for 1.5 h, after that the polymer was precipitate in 500ml cold water and filtration by Buchner funnel, drying and weighted.

Preparation of P MAA-LNPs IPN

1g of MAA (distilled fresh) and 0.5 of LNPs dissolved in 10ml DMF. N, N-methylene bisacrylamide 10% and a trace amount of initiator was add. The mixture placed under a nitrogen atmosphere for half hour to expel dissolved

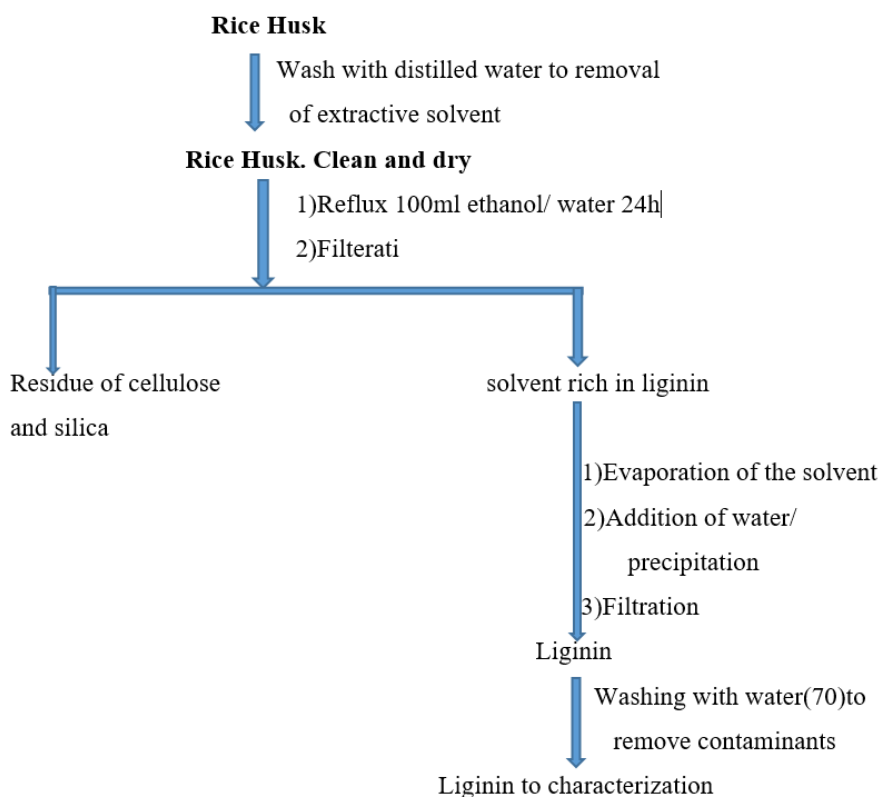
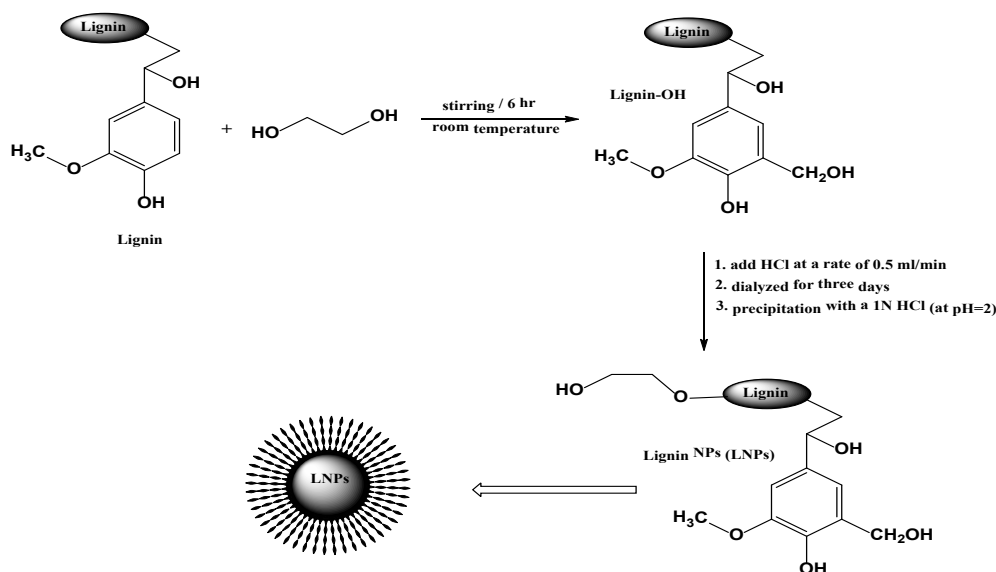
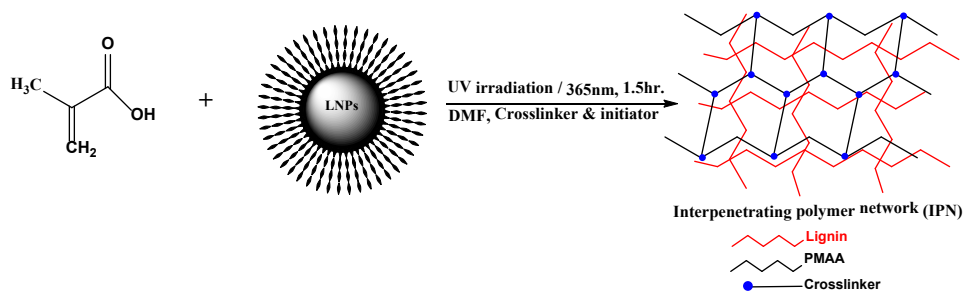


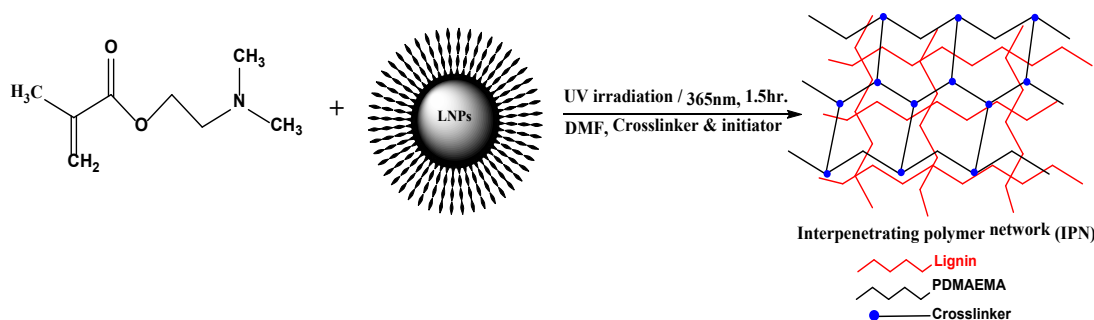
Fig. 2. Flow chart for lignin extraction from rice husk.



Scheme 1. Showed possible reaction mechanism between lignin and ethylene glycol.



Scheme 2. Preparation of PDMAEMA- LNPs IPN.



Scheme 3. Preparation of PMAA- LNPs IPN.

oxygen and placed in UV Irradiation Device (365nm) for Photo polymerization to 1.5 hours. After that, the polymer was precipitate in 300ml cold acidic water and filtration by Buchner funnel, drying and weighted.

Loading the isolated triterpenoid compound on

polymers

Loading isolated triterpenoid compound on PDMAEMA-LNPs IPN

0.18g from the triterpenoid compound isolated and 0.9023g of PDMAEMA-LNPs IPN dissolved in 10ml DCM-Acetone (1:1) by a stirrer to 15 min. preparation 500ml of solution tween 80 (1%)

to precipitation mixture in it. The final mixture placed in stirring 10min and then ultra-sonication 15min. the Precipitate separated by centrifugation 3000 rpm to 45min, drying and Weighted.

Loading the isolated triterpenoid compound on PMAA-LNPs IPN

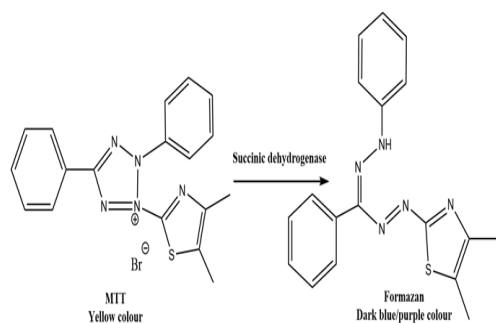
0.53g from PMAA-LNPs IPN and 0.107g of the isolated triterpenoid compound was dissolved in 10ml (DCM: Acetone: methanol) (2:1:2) by a stirrer to 15min. preparation 500ml of solution tween 80 (1%) to precipitation mixture in it. The final mixture placed in stirring 10min and then ultra-sonication 30min. the Precipitate separated by filtration, drying and Weighted.

Anti-Breast cancer activity via MTT assay

Anticancer activities (MTT test) of the compounds and nanoparticles were carried out in Iraqi Biotechnology Co. Ltd., Baghdad, Iraq

Principle

The MTT {3- [4, 5-dimethylthiazol-2-yl]-2, 5-diphenyl-2H-tetrazolium bromide} is a tetrazolium salt dye used in a colorimetric assay, which measures the mitochondrial conversion or modification of the yellow substrate to an insoluble dark blue/purple formazan product. Substrate modification is brought about by the cleavage of MTT by NADH-generating succinic dehydrogenase present in the mitochondria of living cells, with only living cells containing active mitochondria are able to yield a color change. As an increase in mitochondrial enzyme activity leads to a linear increase in the production of formazan dye, the measured quantity of formed formazan dye is directly correlated to the number of metabolically active cells, yielding an accurate measurement of cell viability and thus toxicity (if any). As the formazan dye is insoluble in the reaction medium, it is solubilized by the addition of DMSO or isopropanol and the color intensity is measured spectrophotometrically. as shown in the following reaction [29].



Maintenance of cell culture

MCF-7 cell line was maintained in Rosewell park memorial institute 1640 (RPMI-1640) supplemented with 10% Fetal bovine serum, 100 units/mL penicillin, and 100 µg/mL streptomycin. Cells were passaged using Trypsin-EDTA reseeded at 80% confluence twice a week and incubated at 37 °C [30]. The stock cultures were grown in 25 cm² culture flasks and all experiments were carried out in 96 microliter plates (Gennex Lab, USA).

Procedure

Cell viability was determined by using the 3-(4,5- dimethylthiazol -2-yl) -2,5-diphenyltetrazolium (MTT) on MCF-7 carcinoma. Briefly, 0.1 ml of cell suspension was seeded in 96-well plates (Greiner, Frickenhausen, Germany) with a seeding density of 1×10^4 cells/well. After 24 h or a confluent monolayer was achieved, cells were treated with different concentrations (6.25, 12.5, 25, 50 and 100 µg/mL) of tested compounds and nanoparticles (IDL, B, LNPS, and IML), respectively. Cell viability was measured after 72 h of treated cells by removing the medium, adding 28 µL of 2 mg/mL solution of MTT and incubating the cells for 2.5 h at 37 °C. The colored formazan crystals which were produced from MTT were dissolved in 130 µL of dimethyl sulfoxide (DMSO) followed by 37 °C incubation for 15 min with shaking. The absorbance was measured at a wavelength of 592 nm by ELISA microplate reader [31, 32]. This assay was done in triplicate. The percentage of cell inhibition was expressed by $[1 - (\text{Mean OD of individual test group} / \text{Mean OD of the control group})] \times 100$.

For visualizing the shape of cells under an inverted microscope, 200 µL of cell suspensions, were seeded in 96-well micro-titration plates at density 1×10^4 cells mL⁻¹ and incubated for 48 h at 37 °C. Then the medium removed and added different concentrations (6.25, 12.5, 25, 50 and 100 µg/mL) of tested compounds and nanoparticles (IDL, B, LNPS, and IML), respectively. After 24 h, the plates were stained with 50 µL with Crystal violet and incubated for 15 min at 37 °C, the stain was washed gently with tap water until the dye was removed. The cell was observed under an inverted microscope at 100x magnification microscope filed and photographed with a digital camera [33].

Statistical analysis

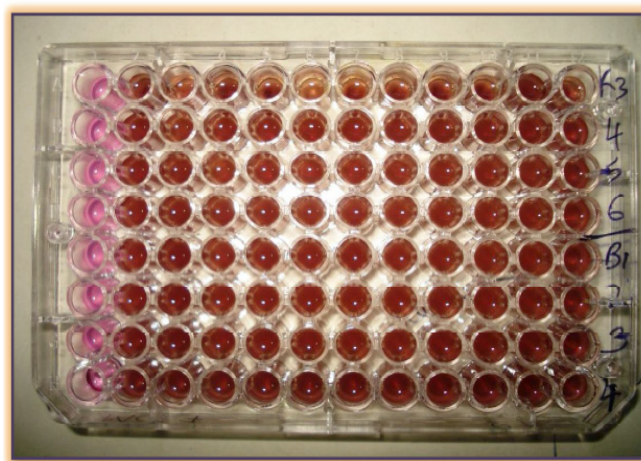


Fig. 3. 96–well plate for cytotoxicity MTT assay.

The obtained data were analyzed statistically using an unpaired t-test with Graph Pad Prism 6. The values were presented as the mean \pm SEM of triplicate measurements.

Results and Discussion

Extracts of *Calotropis Procera L. Leaves*

Table 1 indicates results of percentages of *Calotropis procera L.* leaves extracts; it is observed that ethanolic extract has higher extraction percentage than other extracts. These results may be due to ethanol represent a good solvent to a lot of polar components such as flavonoids, glycosides, saponins, tannins, phenols and other from the polar compound[34]. Among the isolated components of the ethanolic extract, the glycosides occupy the highest ratio due to leaves of *Calotropis procera L.* rich from glycoside compound[35].

Phytochemical Analysis of *calotropis procera L. Leaves Extracts*

Preliminary Phytochemical analysis

Preliminary Phytochemical analysis for petroleum ether (40-60 °C) extract and ethanolic (70%) extracts of *C.procera L.* leaves were performed using qualitative chemical tests and the results were tabulated in Tables 3.2. The results showed the ethanolic (70%) extract is rich in popular phytochemical constituents such as glycosides, flavonoids, saponin, phenolic compounds, and tannins. While petroleum ether (40-60 °C) extract has fewer chemical families, the reason back to selective petroleum ether to the polarity medium components, for example, triterpenoids. These findings are in agreement with the results of [36-38].

Thin Layer Chromatography (TLC)

The result presented in Fig. 4. show that the

TABLE 1. Seed extracts *calotropis procera L.* leaves.

Extract's type	Percentage	Nature of substance
	(%)	
In Ground leaves		
Oil	2.5595	Dark green- viscous
Ethanolic extraction	20.35975	Black garbage
Flavonoid	11.678	Black
Glycosides	56.064	Solid- yellow dark shiny
Saponin	3.016	Green harry for black

TABLE 2. Results of Preliminary Phytochemical analysis of calotropa procera leaves

No.	Chemical Test	Extracts	
		Petroleum ether	Ethanol 70%
1	Test for Carbohydrates and glycosides: a) Molisch	+	+
	b) Benedict: 1- Before analysis	+	+
	2-After analysis	+	+
2	Test for amino acids and proteins: Biuret	-	-
3	Test for Triterpenoids and Steroids: a) Salkowski reaction	+	-
	b) Liebermann –Burchard	+	+
4	Test for Flavonoids: a) Ethanolic KOH	-	+
	b) Magnesium turnings	-	-
5	Test for Alkaloids: a) Dragendroff	-	-
	b) Wagner	-	-
	c) Marquis	-	-
6	Test for Tannins and Phenolic compounds: Lead acetate sol.	+	+
7	Test for Saponins: a) Foam test	+	+

petroleum extract of *Calotropis procera L.* leaves comprises two components. ($R_f = 0.05$ and 0.64) of these components are regarding the triterpenoid family because of giving a positive test with the special reagents. Moreover, the results

revealed that the isolated compound by column chromatography technique is one compound with R_f value of 0.1 relationship to the triterpenoid family.

Infrared spectrum of the isolated compound from

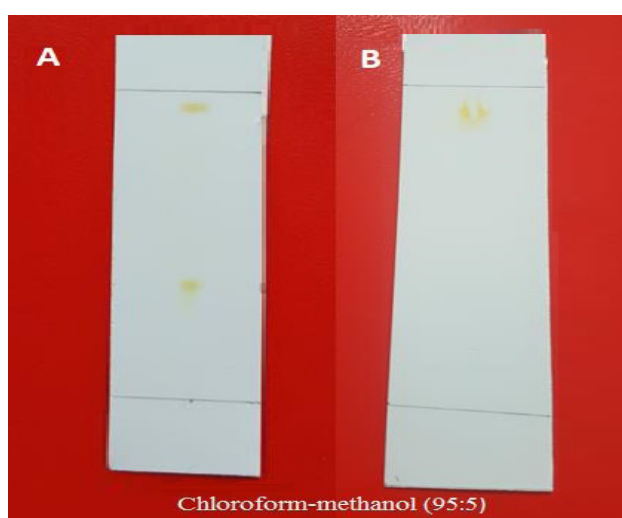


Fig. 4. Thin layer chromatography of (A) extract after saponification processing and (B) Isolated compound extract from column from *calotropis procera L.*

TABLE 3. The major IR bands to isolated compound from *Calotropis Procera* L.

Frequency (cm ⁻¹)			
Str.			
O-H	C-H	C=O	C=C
3375.54	2928.04	1728.28	1458.23

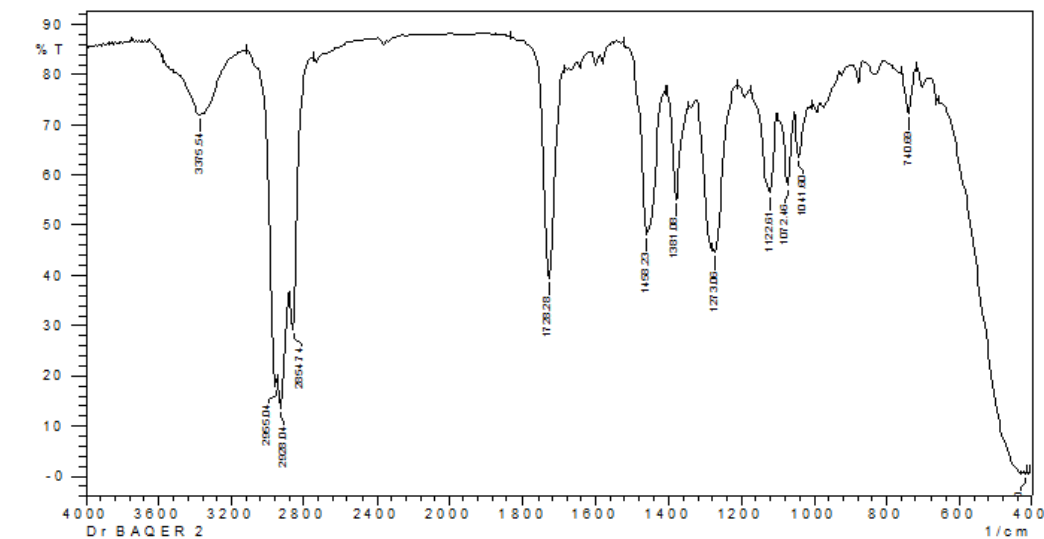


Fig. 5. FTIR Spectrum of isolation compound

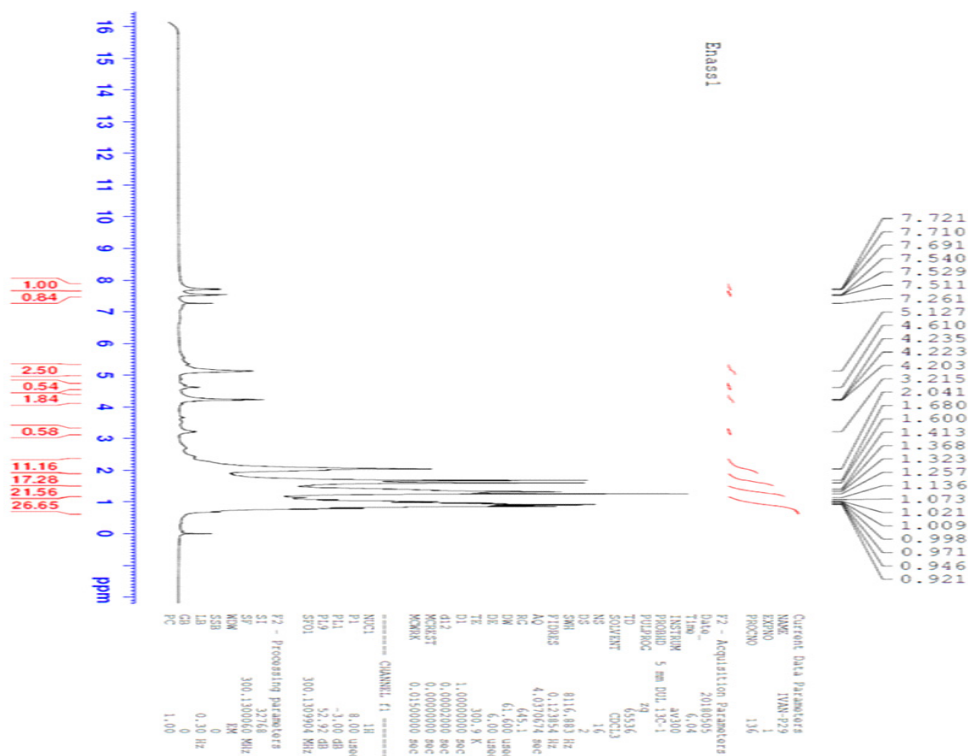


Fig. 6. ¹H-NMR of isolation compound from *calotropis procera* L.

Calotropis Procera L.

IR spectrum of isolation compound shows absorption bond in 3375.54 cm^{-1} that back to a hydroxyl bond absorbent. In addition, absorption bonds in $(2955.04, 2928.04)\text{ cm}^{-1}$ and 2854 cm^{-1} indicated to the absorbent cycloalkane, CH_2 , and methylene group on respectively. On another hand, the bond 1728.28 cm^{-1} referred to the present $\text{C}=\text{O}$ group.

¹H-NMR and ¹³C-NMR Spectrum of the isolated compound from Calotropis Procera L.

The isolated compound was subjected to ¹H-NMR and ¹³C-NMR spectrum and the spectrum as shown in Fig. 6 - 9, respectively. ¹H-NMR spectra showed peaks at δ_{H} corresponding to H-6 of an olefin proton, δ_{H} 3.21 to H-3 in addition to six methyl group singles at δ_{H} 1.00, 0.92 (s each, Me-19, -18), 0.98, 0.97, 0.94 (d each Me-21, 26, 27) and 0.87 (t- Me-29). ¹³C-NMR showed a number of signals including six methyls (CH_3),

eleven methylenes (CH_2), nine methane (CH) and three quaternary carbons (C). The signal at δ 29.0 and 26.54 corresponds to an angular carbon atom (C_{19} & C_{18}). The aforementioned data with the ¹³C-NMR indicated the presence of triterpene compound[39].

Infrared spectrum of natural polymers Lignin, LNPs and IPNs

Functional groups are pointed at Table 4. The softwood lignin is normally characteristic higher intensity of the band at 1512 than 1581 cm^{-1} [28]. We note that there are no other residues of carotid residue and residues of polysaccharides that have a bending band at 1205 cm^{-1} [40]. The variation between the lignin and LNPs can be observed from the shifting of the peak from 1708 to 17012 cm^{-1} as well as 3446 to 3444 because of increase polar group (OH) in LNPs. The lowering in the value of absorption characteristics to the aromatic ring can be correlated with the participation

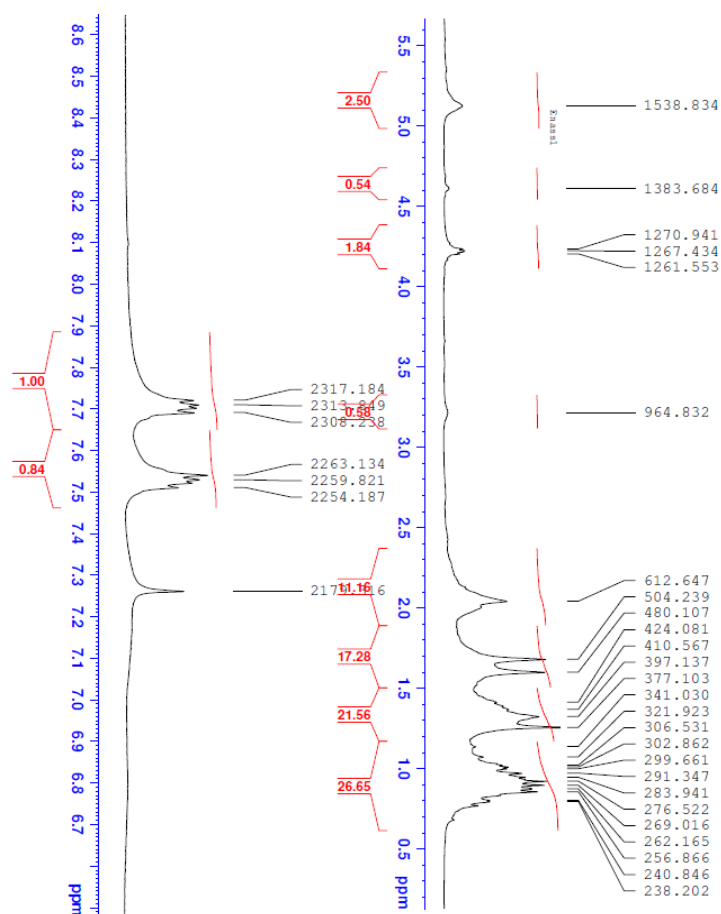
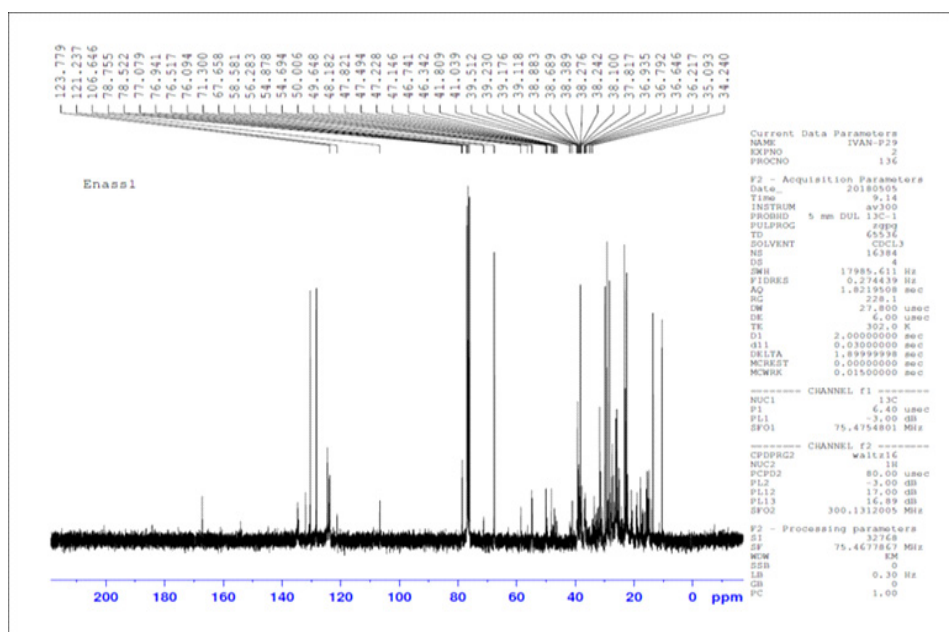
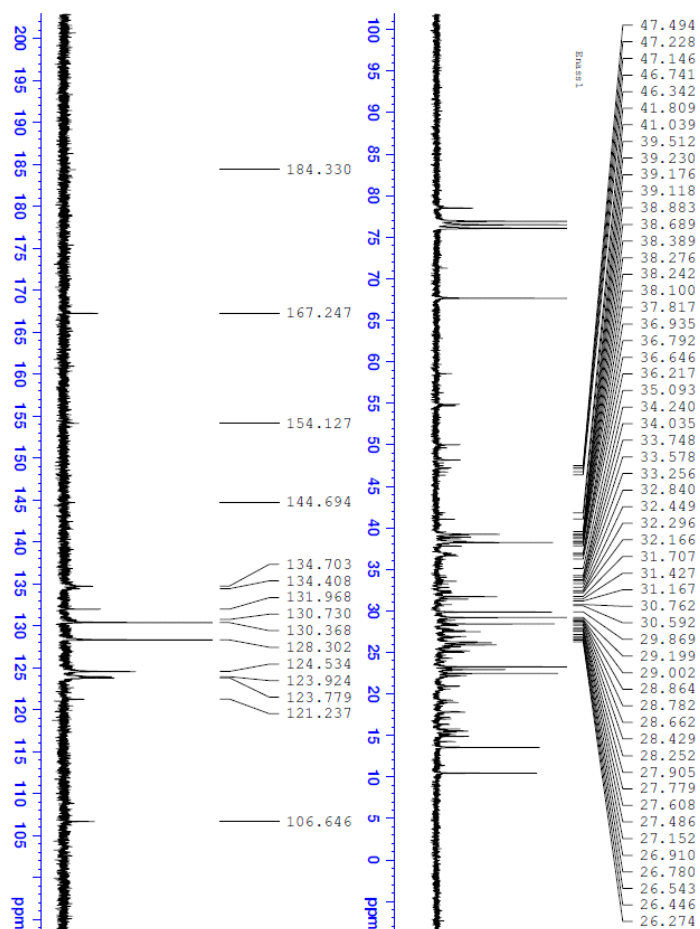


Fig. 7. Expanded ¹H-NMR of isolation compound from calotropis procera L

Fig. 8. ^{13}C -NMR of isolation compound from *calotropis procera* L.Fig. 9. Expanded ^{13}C -NMR of isolation compound from *calotropis procera* L.

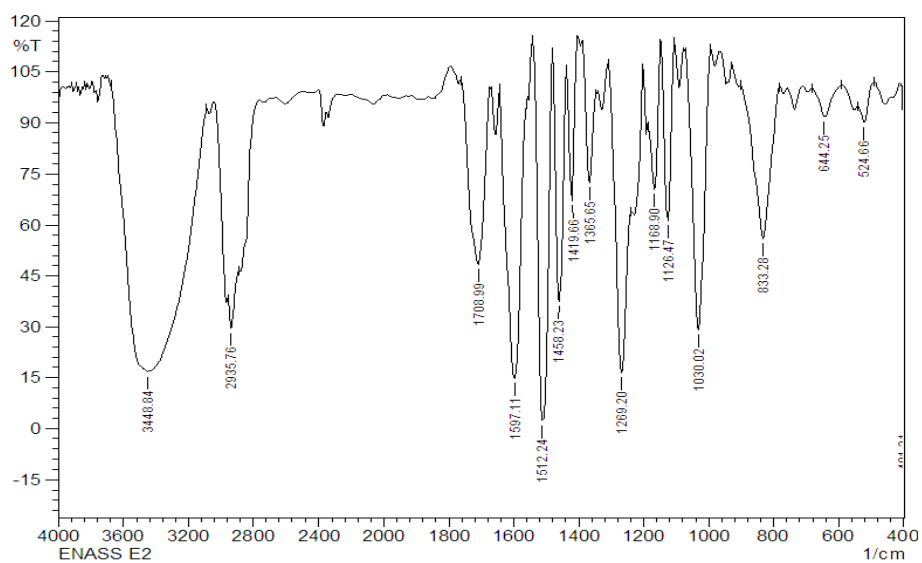


Fig. 10. FTIR Spectrum of Lignin.

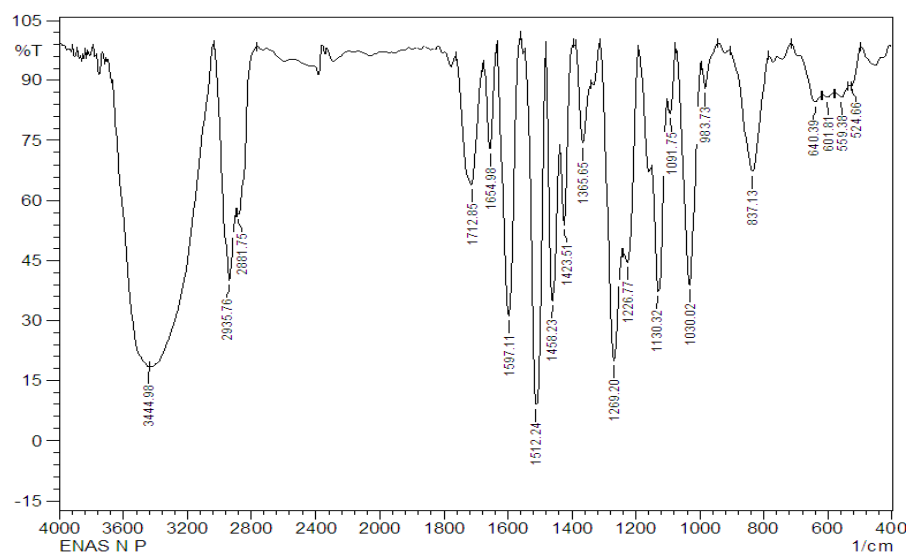


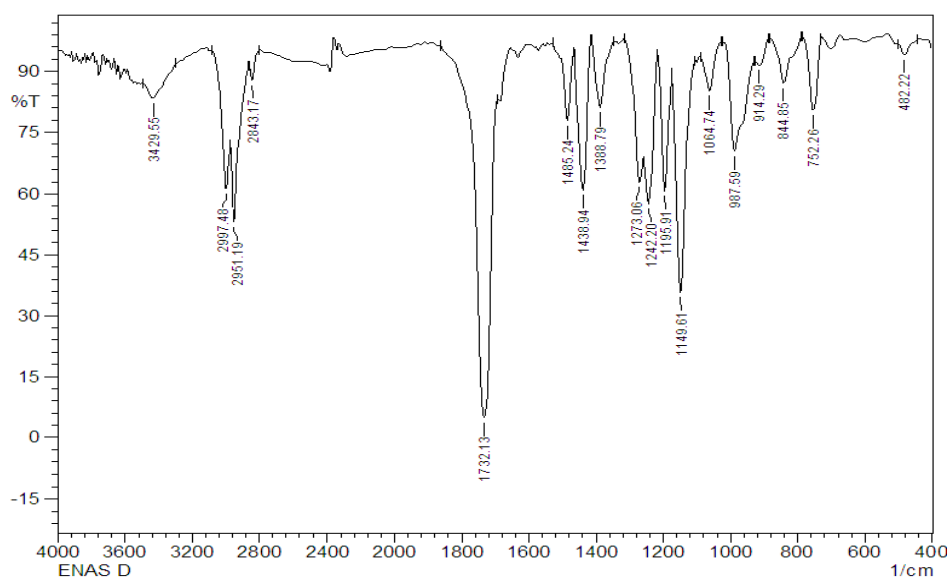
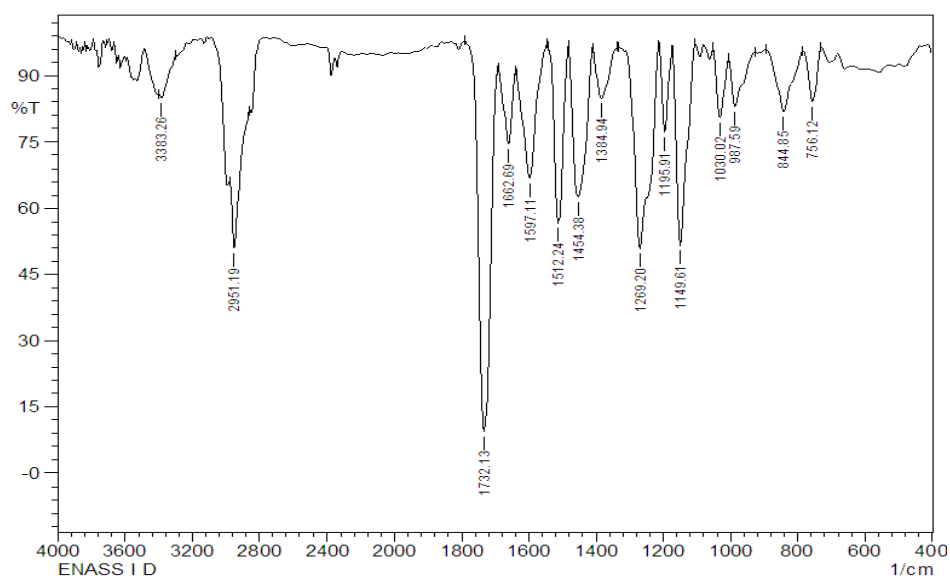
Fig. 11. FTIR Spectrum of LNPs.

TABLE 4. The major IR bands to lignin and LNPs

Polymers Code	Frequency (cm ⁻¹)Str.				
	O-H	C-H	C=O	C-O-C	C=C (Aromatic)
Lignin	3448.84	2935.76	1708.99	1126.77	1512.24 & 1600.97
LNPs	3444.98	2935.76	1712.85	1130.32	1512.24 & 1597.11

TABLE 5. The major IR bands to PDMAEMA, PDMAEMA-LNPs IPN, and PDMAEMA-LNPs IPN after loading

Polymers Code	Frequency (cm-1) Str.		
	N(CH ₃) ₂	C=O	C-N
Poly(DMAEMA)	2951.19	1732.13	1149.61
Poly(DMAEMA)-LNPs IPNs	2951.19	1732.13	1149.61
Poly(DMAEMA)-LNPs IPNs after loading	2931.90	1732.13	-

**Fig. 12.** FTIR Spectrum of PDMAEMA**Fig. 13.** FTIR Spectrum of PDMAEMA-LNPs IPNs

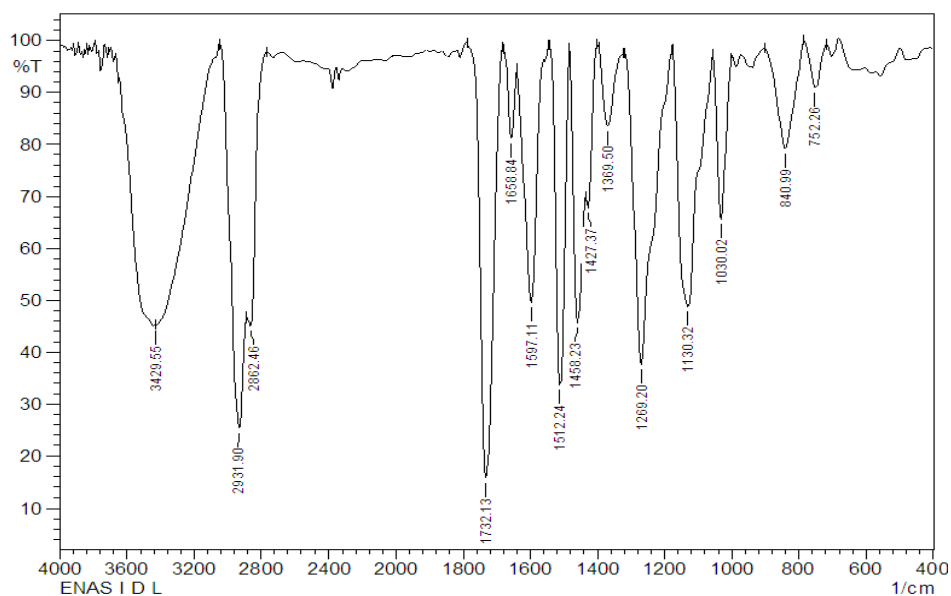


Fig. 14. FTIR Spectrum of PDMAEMA-LNPs IPNs after loading

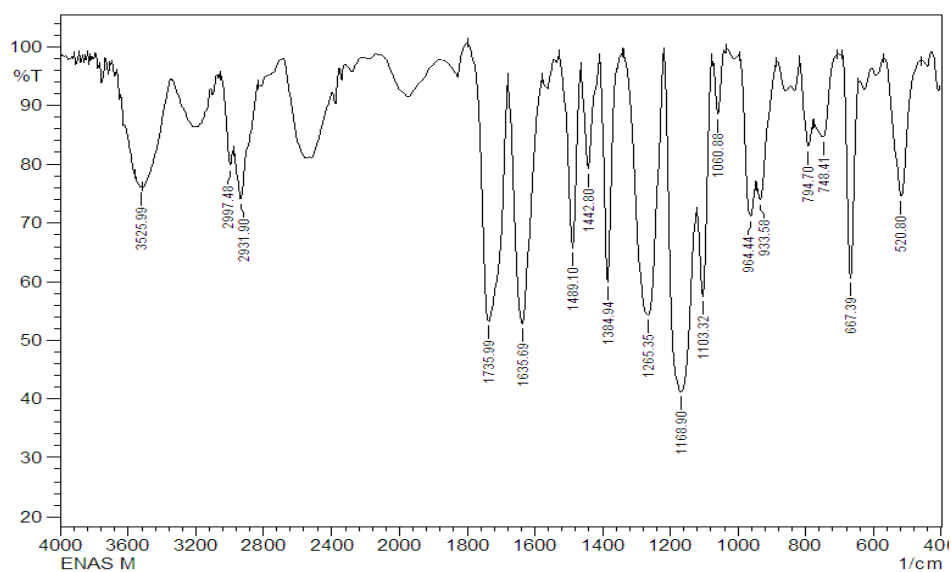


Fig. 15. FTIR Spectrum of PMMA.

TABLE 6. The major IR bands to PMAA, PMAA-LNPs IPN, and PMAA-LNPs IPN after loading.

Polymers Code	Frequency (cm ⁻¹) Str.		
	O-H	C-H	C=O
Poly(MAA)	3525.99	2997.48	1735.99
Poly(MAA)-LNPs IPN	3444.98	-	1724.42
PMAA-LNPs IPN after loading	3441.12	-	1728.28

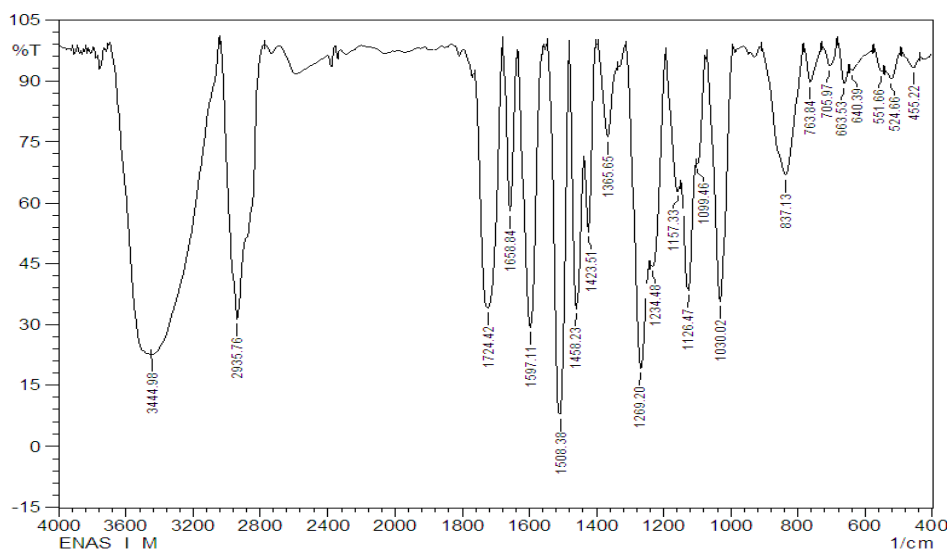


Fig. 16. FTIR Spectrum of PMMA-LNPs IPNs

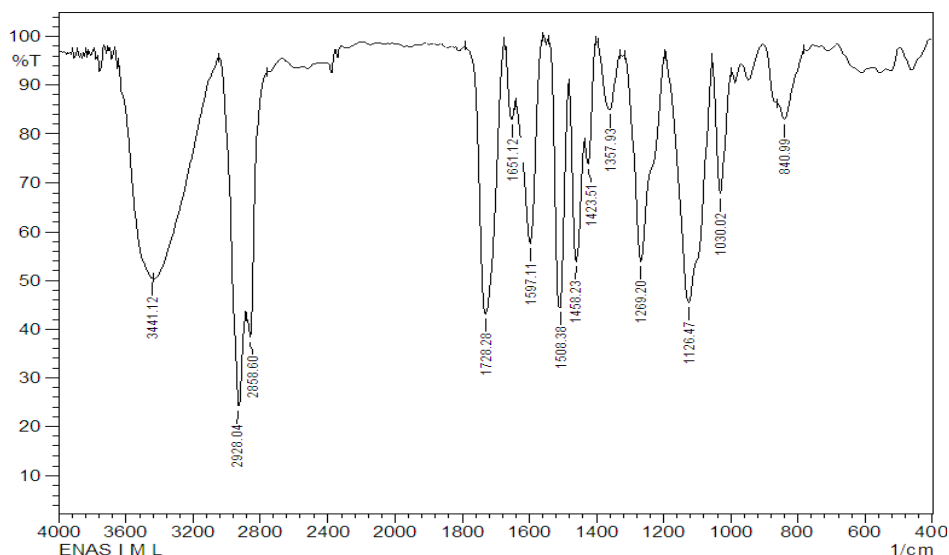


Fig. 17. FTIR Spectrum of PMMA-LNPs IPNs after loading

of structural units of lignin in substitution and condensation reactions and the mood for obtaining nanoparticles[28], revealed from the FTIR investigation, that the chemical compositions of the lignin and LNPs are similar and characteristics peaks are margin different. The IR spectra of Lignin and LNPs are shown in Fig. 10 and 11 respectively. The Poly(DMAEMA)-LNPs IPN spectrum shows the existence of a 1732cm^{-1} C=O bond belonging to the DMAEMA, and 1149.61cm^{-1} to stretching C-N. The bond of LNPs such as 1512.24cm^{-1} to the aromatic ring, and 1030.02cm^{-1} to C-O alcohol[41]. We observe a decrease in intensity bonds to polar groups returning to LNPs

due to overlaps intra IPN. Figures 12-14 represent FTIR spectra for these prepared polymers, and selected characteristic bands and their locations are shown in Table 4.

We observe from Table 5 a slight shifting in the main bond positions after preparation IPN and after loading. The disappearance of the bound 2997.48cm^{-1} package to MAA due to lack of concentration in the resulting network. The bundles of the aromatic rings (1512.24 to 1508.38) and some other groups (1130.32 to 1126.47) it's returning to LNPs reducing their intensity with little displacement because of increased interference between the polyacrylate and LNPs,

Fig. 14-16 represent FTIR spectra for these prepared polymers.

Thermal Gravimetric Analysis(TGA)

Quantitative thermal analysis is a technique for measuring the mass of a substance as a function of temperature or time in the presence of an inert atmosphere such as nitrogen or helium. The substance suffers from loss or increase in weight under the influence of heating or cooling in the oven. In often the thermal stability of new polymeric material in inert and oxidizing atmospheres form a major concern. TGA is well suited to we enable to gain information about the inclination of a polymer to degrade under these

conditions[42]. the aim of the thermal analysis study is finding a kinetic modal to calculating many of parameters as activation energy, enthalpy, $\ln[-\ln y] = -\frac{Ea}{RT}$ the parameters are very important to help in understanding the behavior of the materials in high temperatures. The Broido1969 method is used to calculate the activation energy according to the following equation:

$$\text{Where: } y = \frac{W_t - W_\infty}{W^o - W_\infty}$$

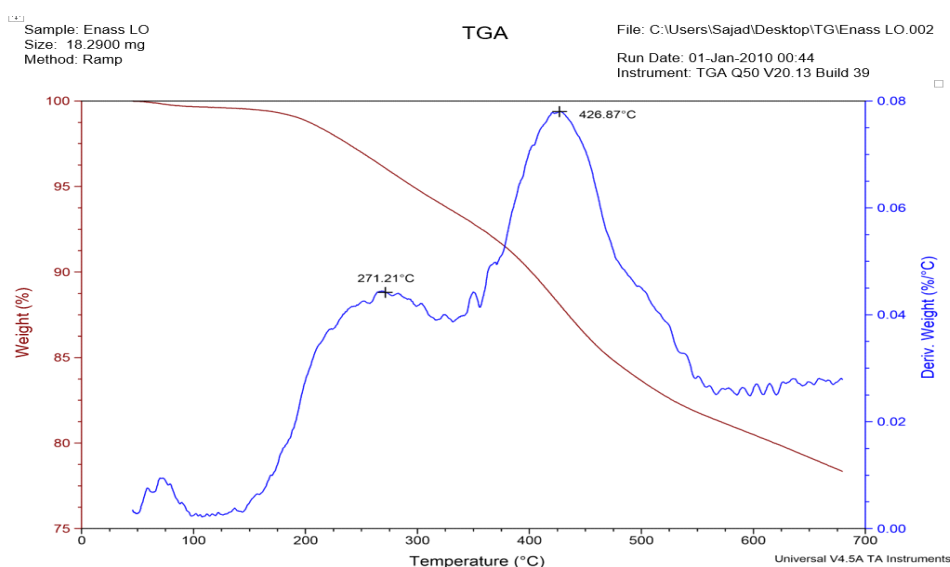


Fig. 18. TGA thermogram of lignin.

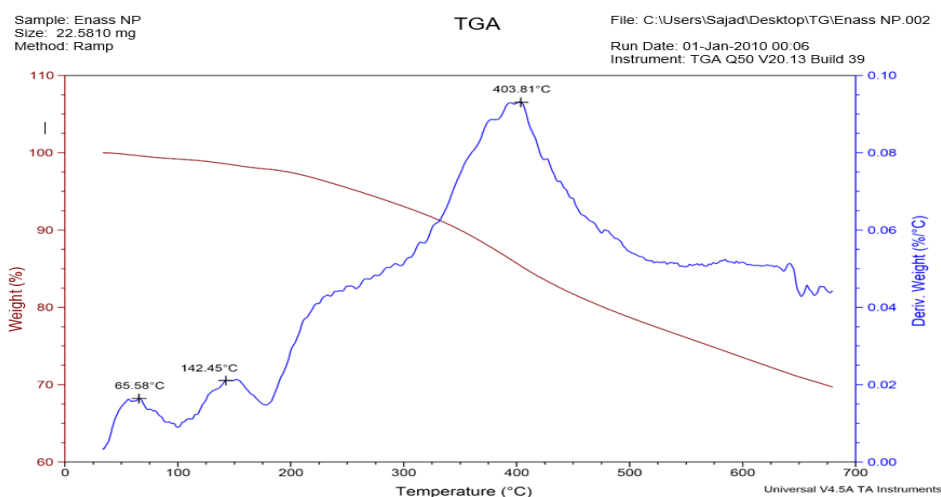


Fig. 19. TGA thermogram of LNPs.

Where y is the fraction of a number of initial molecules not yet decomposed; W_t represents Weight at any time t ; W_{∞} represents weight in total final time and the initial Weight. A plot of $\ln(y/(1-y))$ vs $1/T$ gives a straight line. The slope is related to activation energy E_a [43]. TGA was measured in temperature range 25-700°C, constant heating rate 50°C/min at N₂

atmosphere.

Thermal Gravimetric Analysis(TGA) of lignin and LNPs

Figures 18 and 19 show the TGA thermograms for lignin and LNPs on respectively and the important thermal stability functions for this figures explained in Table 7, display good thermal

TABLE 7. Thermal stability functions of all prepared polymers.

Polymer code	Decomp. Stage	T _i (°C)	T _f (°C)	Activation Energy kJ.mol ⁻¹	Temp. Range for Activation Energy(°C)	weight loss %	Temp. of 50% weight loss(°C)
Lignin	1 st decomp.	155	335	98.61962	155-221	93.4	408
	2 st decomp.	363	570	266.9098	363-406	81.2	
LNPs	1 st decomp.	202	275	50.29214	202-280	94	350
	2 st decomp.	324	548	207.776	324-362	76	
Poly (DMAEMA)	1 st decomp.	261	373	154.1442	261-298	79	336
	2 st decomp.	395	496	252.71	395-427	69.4	
Poly (DMAEMA)-LNPs IPNs	1 st decomp.	233	290	75.804	233-274	69.7	430
	2 st decomp.	265	565	170.026	365-400	71	
Poly(MAA)	1 st decomp.	189	340	99.6622	189-208	78.2	465
	2 st decomp.	424	550	118.784	424-520	48	
Poly(MAA)-LNPs IPNs	1 st decomp.	223	340	124.492	223-258	93.7	416
	2 st decomp.	373	610	149.4255	373-404	80	

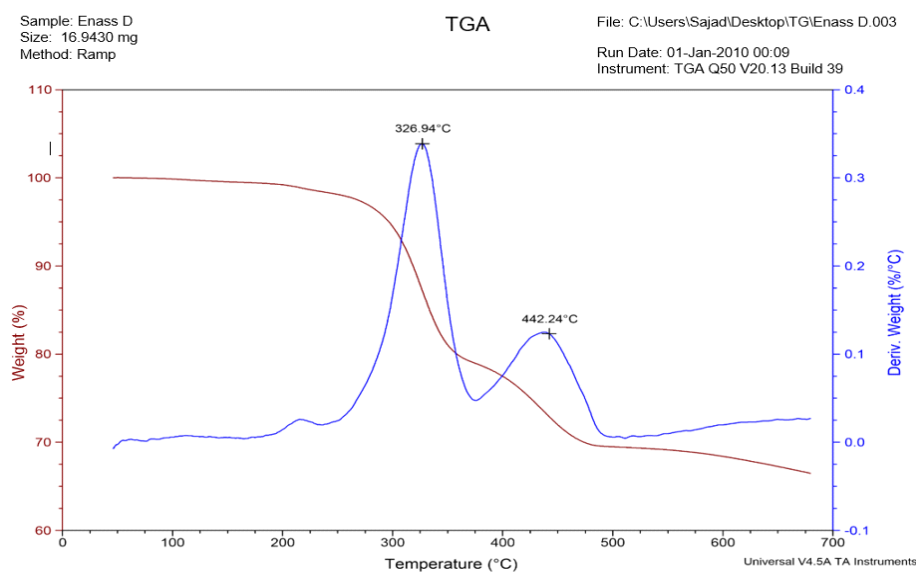


Fig. 20. TGA thermogram of PDMAEMA

stability resulting from the presence of aromatic rings. Lignin has a broad temperature range (100-700)°C during thermal degradation due to structure contrast in started units of lignin. in TG curve lignin, the weight-loss can be observed in Several stages. Initially, Moisture removal and volatilization of products that low molecular weights such as CO₂ and CO occur even 200°C. a release of methyl, ethyl, and vinyl guaiacol derivatives occur between 230 and 260°C

resulted from degradation of propanoid side chains of lignin[44]. We Observe from LNPs curve increased ($T_i=202^\circ\text{C}$) value, that gives to LNPs higher thermal stability compared with lignin. in addition, decrease weight loss during another decomposition stages because of existing

Thermal Gravimetric Analysis of Poly(DMAEMA) and Poly(DMAEMA) – LNPs IPNs

TGA curve of Poly(DMAEMA) exhibit high

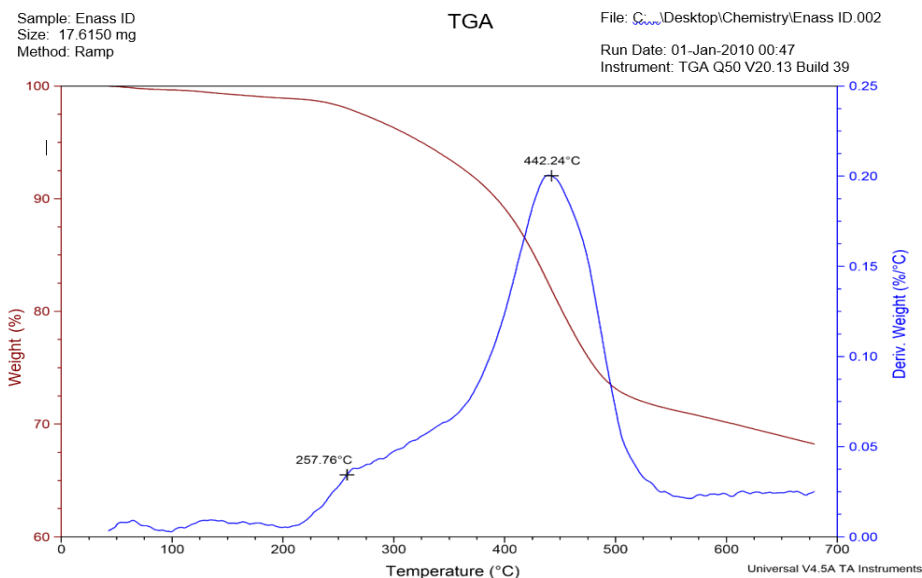


Fig. 21. TGA thermogram of PDMAEMA-LNPs IPNs.

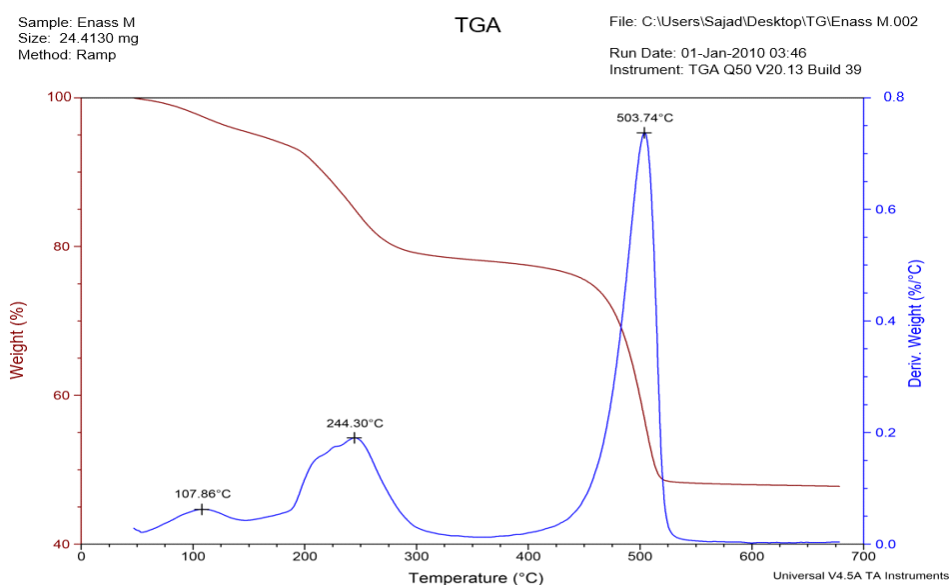


Fig. 22. TGA thermogram of PMAA.

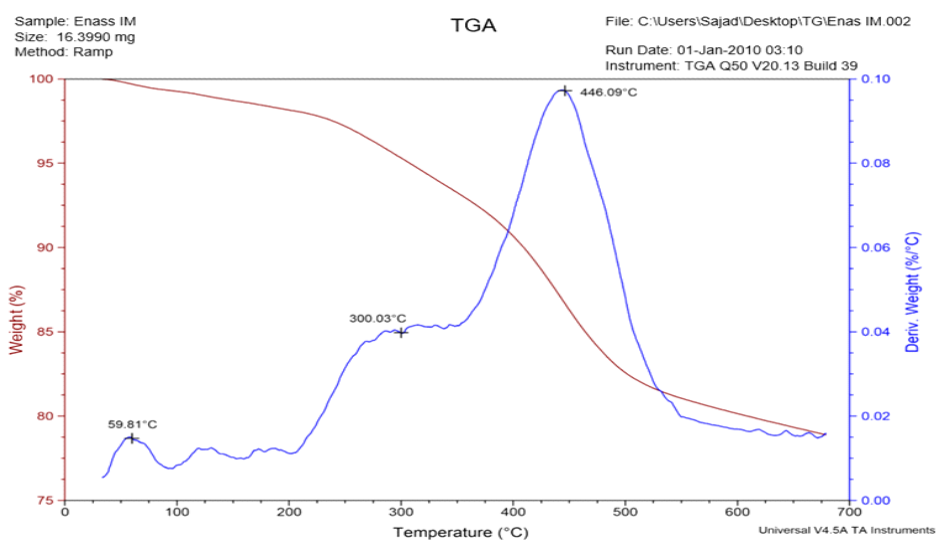


Fig. 23. TGA thermogram of PMAA-LNPs IPNs.

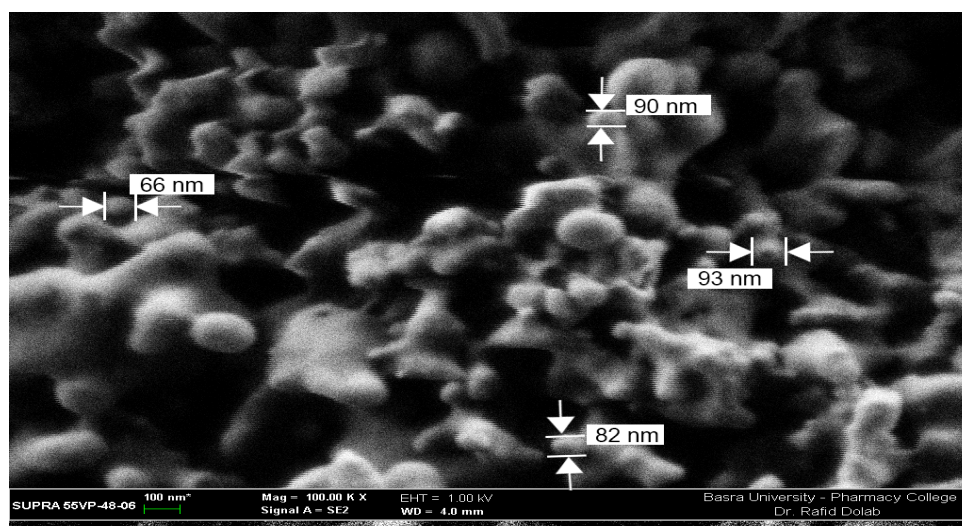


Fig. 24. SEM of LNPs in 100nm

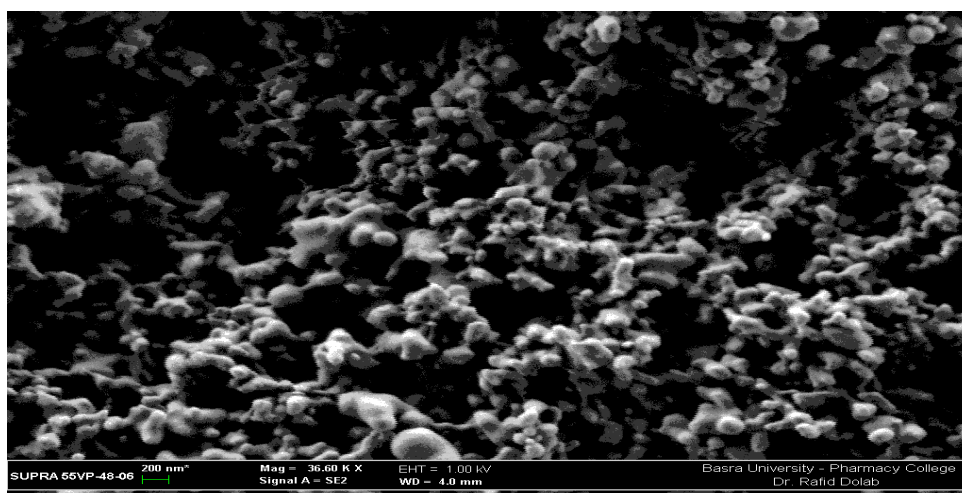


Fig. 25. SEM of LNPs in 200nm

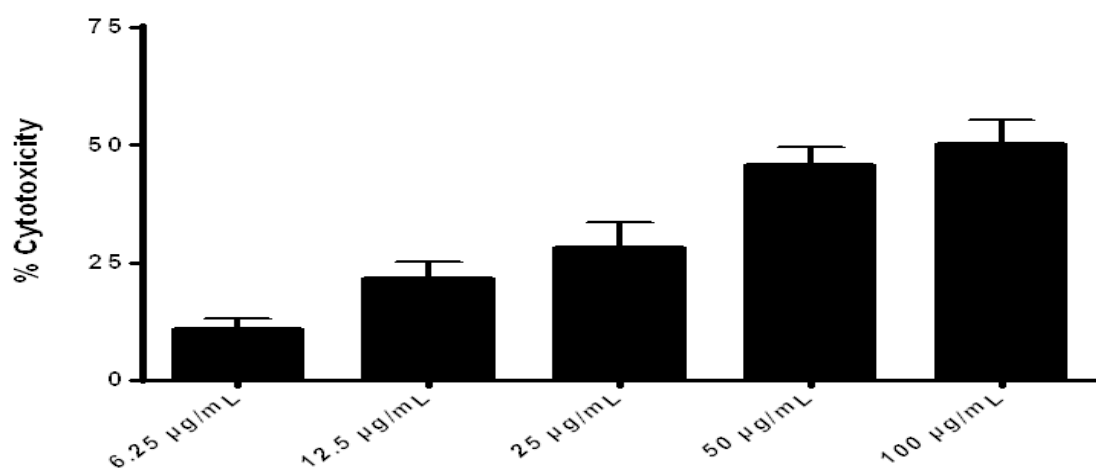


Fig. 26. Cytotoxic effect of (B) in MCF-7 cells

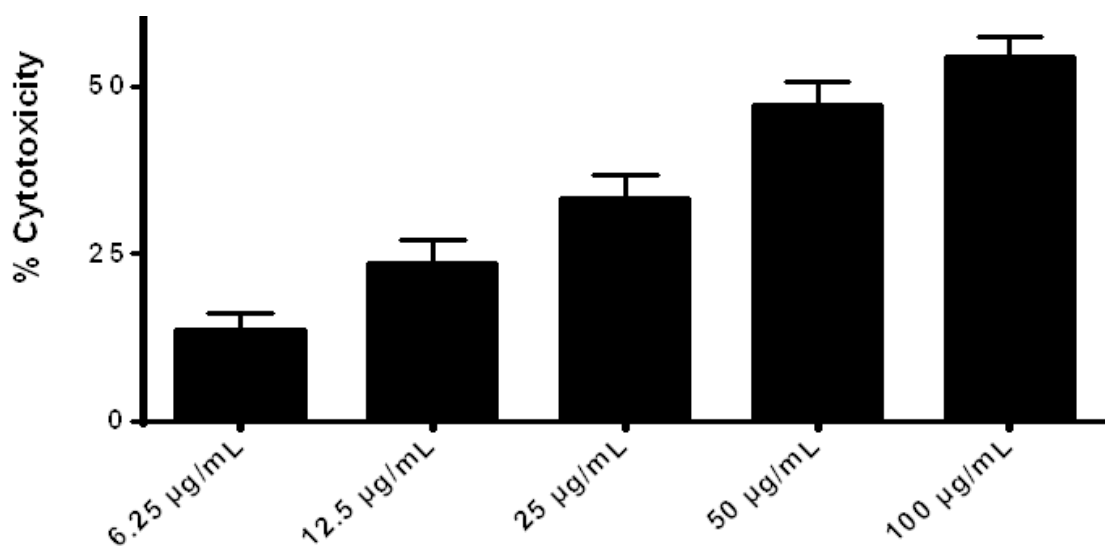


Fig. 27. Cytotoxic effect of (LNPs) in MCF-7 cells

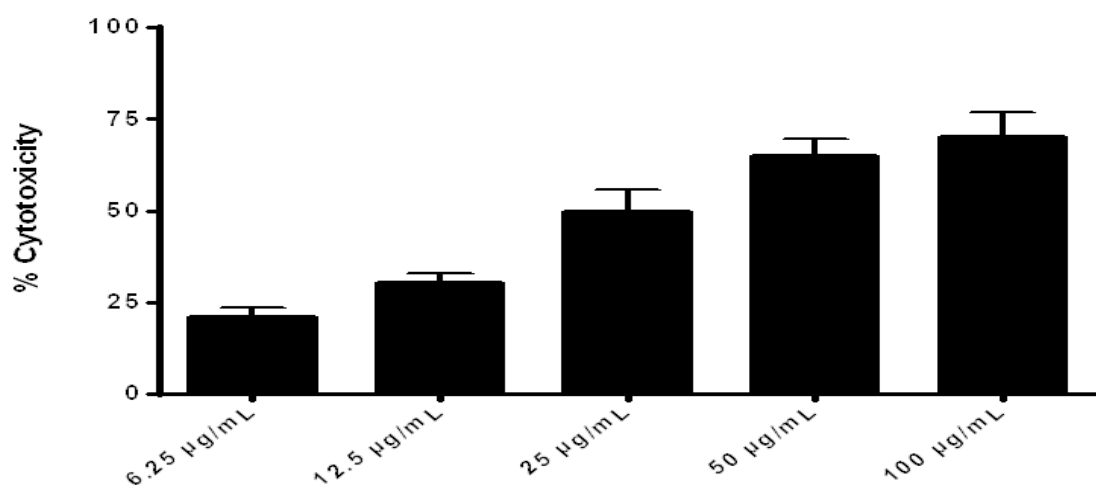


Fig. 28. Cytotoxic effect of (IDL) in MCF-7 cells.

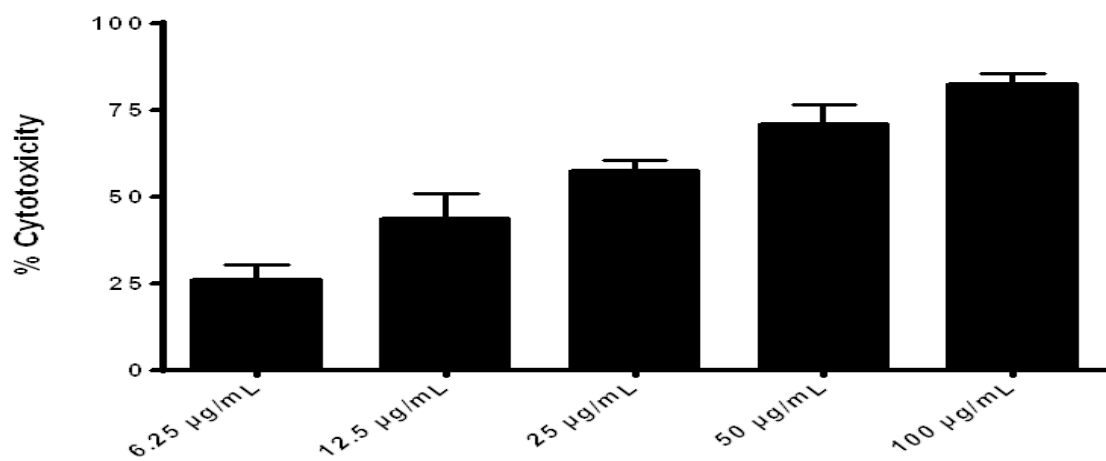


Fig. 29. Cytotoxic effect of (IML) in MCF-7 cells

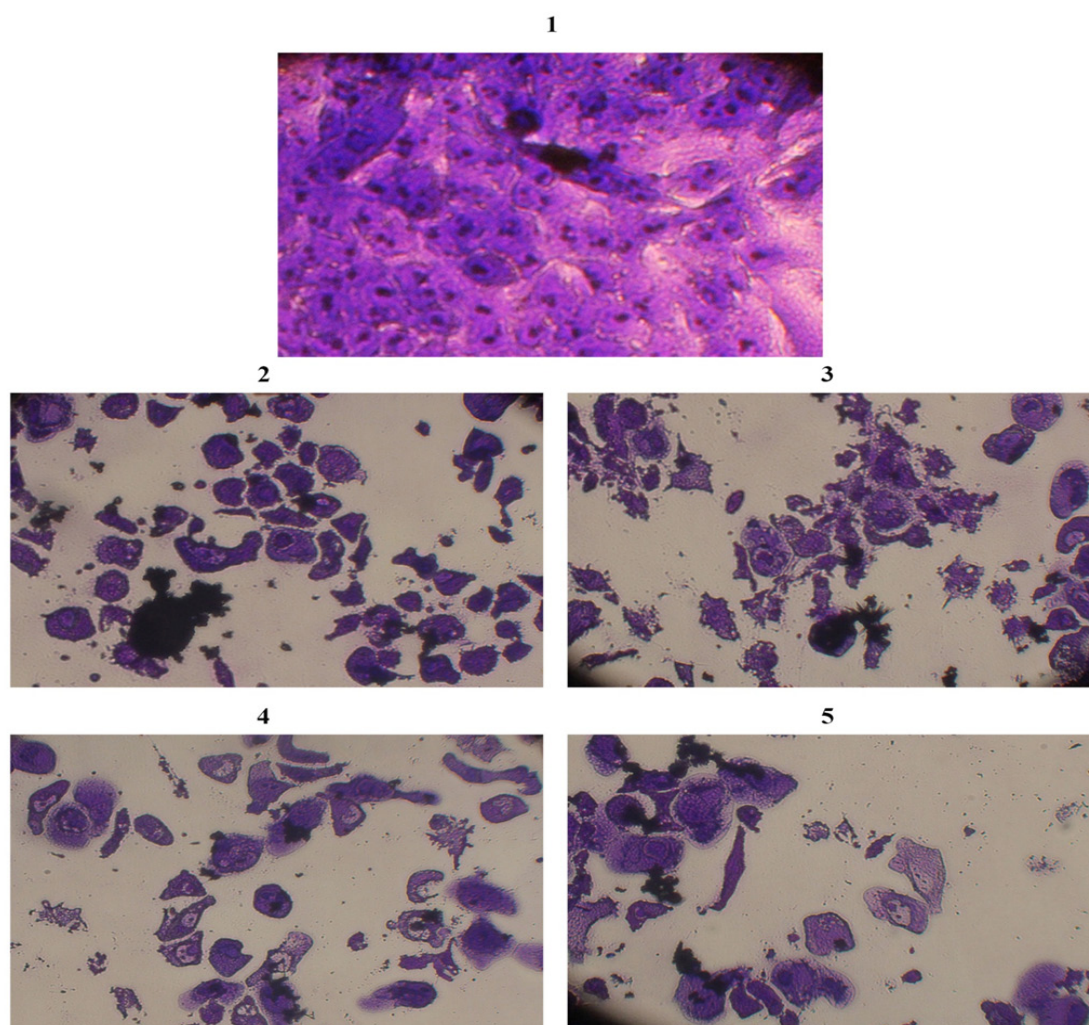


Fig. 30. Anti-proliferative activity of tested components against MCF-7 cells. 1, control untreated cells. 2, Cells were treated with A. 3, Cells were treated with B. 4, Cells were treated with IDL. 5, Cells were treated with IML.

thermal stability up to (261°C) and weight loss is no great until (300°C) as shown in Fig. 20. Poly(DMAEMA) suffers large loss weight percent in the first stage, that loss is back to decomposition the longer lateral chains of dimethyl amino ethyl groups from P(DMAEMA)[45]. Figure 21 shows increase thermal stability, dramatically reduce from weight loss through all decomposition stages and an increase in the decomposition temperature range, with reason existence LNPs aggregation within the network structure.

Thermal Gravimetric Analysis (TGA) of Poly(MAA) and poly LNPs-(MAA) IPNs

The PMAA Stabilization showed up (200°C). Then showed the analysis in two stages, the weight loss in the second stage is greater than the first stage. Where they suffer the loss of side chains at the first stage. The prepared network presents thermal stability due to the presence of tangles and the resulting aggregations due to the presence of the LNPs.

Scanning Electron Microscopy (SEM)

The examination of the morphology and nanoparticles geometry of the prepared LNPs was performed by using SEM at different amplifications (200 nm and 100 nm).

From Fig. (3.24) and (3.25), the size of the nanoparticles was found to be in the range of (66-93) nm.

Anti-breast cancer activity

The toxicity associated with cancer chemotherapy arises primarily from the lack of specificity for tumor cells. To handle this problem, the focus of many studies is on natural compounds that inhibit cancer cells more selectively than normal cells[46]. Therefore, the interest in the pharmacological effects of bioactive compounds on cancer treatments and prevention has increased dramatically over the past twenty years. It has been shown to possess numerous anti-cancer activities in various cancer cells through different forms of cytotoxic effects without exhibiting considerable damage to normal cells [47]. Today, medicinal plants constitute a common alternative for cancer prevention and treatment in many countries around the world. Approximately, 60% of the anti-cancer drugs currently used have been isolated from natural products from the plants. At this time, more than 3000 plants worldwide have been reported to possess anti-cancer properties [48].

The traditional usages of plants containing triterpenoids in folk medicine are multiple, in terms of anti-inflammatory, hepatoprotection, analgesia, cardiotoxic, sedative and tonic effects, etc. Many of these therapeutic effects have been confirmed by contemporary scientific research [49]. Recent evidence supports the beneficial effects of naturally occurring triterpenoids against several types of human diseases, including various types of cancers. Anticancer potential of triterpenoids and their anti-inflammatory, antiproliferative, and pro-apoptotic effects have been investigated both in *in vitro* and *in vivo* models [50]. MTT assay is a universally accepted *in vitro* method for screening the drugs having cytotoxic activity. It is a colorimetric assay based on a color change by metabolically-active cells. *In vitro* cytotoxic activity against MCF-7 cell line at different concentrations of B, LNPs, Poly(DMAEMA)-LNPs IPNs after loading (IDLNPs), and Poly(MAA)-LNPs IPNs after loading (IMLNPs) were studied for 72 h. In the present study, MCF cells showed growth inhibition in a dose-dependent manner when treated with tested compounds and nanoparticles (triterpenoid isolated compound (B), LNPs, IDLNPs and IMLNPs) at concentrations ranging from 6.25 µg/mL-100 µg/mL, as shown in Fig. 26 to 29. At the high concentration (100 µg/mL), the result revealed that IMLNPs had a significant ($p < 0.01$) higher cytotoxicity on MCF-7 cell line followed by IDLNPs and LNPs while triterpenoid isolated compound (B) had the least. The percentage of dead cells for each tested compounds at the higher concentration was found to be 50.31, 54.43, 70.42 and 82.67, respectively. The 50% cytotoxic effect (IC_{50}) of IMLNPs was found to be 66.07. In our study, we showed that significant inhibition of MCF-7 proliferation after 72 h. The cell proliferation was significantly lower compared to the untreated control cells. After 72 h of treated with triterpenoid isolated compound (B) at the concentration of 6.25 µg/mL, there was low cytotoxicity on MCF-7 cell line while LNPs at the same concentration showed moderate cytotoxic effects on the cell line. IDLNPs and IMLNPs at the concentration of 6.25 µg/mL killed >25% of the cells. The results indicate that these compounds are potential sources of effective antiproliferative and cytotoxic substances. The apoptogenic property of the compounds was investigated

through morphological changes on the MCF-7 cell line using an inverted phase contrast microscope. As seen in Fig. 30, the control (untreated) cells maintained their original morphology and were mostly attached to the tissue plate. Contrarily, treated with LNPs exhibited low efficiency on the morphology of the cells. Treated with, IDLNPs and IMLNPs exhibited high antiproliferation activities and morphological variations on the cells after 72h. Typical apoptotic features such as membrane blebbing and loss of contact with adjacent cells were observed; the number of cells was also decreased. This suggests that the nanoparticles have the potential for in vivo applications [51]. At the maximum concentration of IMLNPs, none of the cells survived confirming its anti-cancer property. The probable reason might be by inhibiting cell proliferation and finally killing the cells which were well implicated by the absence of Formosan crystals in the dead cells. The cell death suggesting that IMLNPs could be a good cytotoxic agent. The well-defined pathological changes such as giant cell formation, rounded and shrunken appearance of cells, particulate and vacuolated structure, grouping and peeling of monolayer observed on IMLNPs further confirmed the compounds potential as a cytotoxic agent against the MCF-7 cell line [50].

Conclusion

The present study is shown that *Calotropis Procera* L. leaves contain the triterpenoid compound. Thus, it may support the ethnobotanical claim of *Calotropis Procera* L. for the treatment of many diseases. also, MCF cells showed growth inhibition in a dose-dependent manner when treated with tested compounds and nanoparticles (LNPs, triterpenoid isolated compound (B), IDLNPs and IMLNPs) at concentrations ranging from 6.25 µg/mL 100 µg/mL. At the high concentration (100 µg/mL), the result revealed that IMLNPs had a significant ($p < 0.01$) higher cytotoxicity on MCF-7 cell line followed by IDLNPs and triterpenoid isolated compound (B) while LNPs had the least. The anti-breast cancer activity exerted by the IMLNPs may be in part due to the presence of a synergistic effect of the triterpenoid compound and lignin for cytotoxic potency against MCF-7 cells. The present in vitro study lends to support its antiproliferative and anticancer activity. Hence, it can be regarded as

a potent and valuable chemotherapeutic agent in the management of breast cancer. on another hand, the IPNs based on LNPs increases of effect isolated compound and therefore other drugs. IPNs based LNPs shows good thermal stability, this feature allowed to store to an approximately large periodic of time.

Acknowledgments

The Thanks first and finally to Allah, All Praise is for Allah by whose favor good works are accomplished. We sincere gratitude to for all workers in the department of chemistry/science College and palm research center / Basrah university for allowing to work in the laboratories. We offer thanks to Assist. Prof. Dr. Whidad S. Hanoosh and Prof. Dr. Salah S. Hashim, Assist. prof. Dr. Zaki A. Nasir Al-Shamkhani, Mr. Alaa A. Albaheli, and Dr. Hussein J. Shareef whoever helped us during the course of this work.

References

1. Chassenieux, C., et al., Biopolymers: State of the art, new challenges, and opportunities. *Handbook of Biopolymer-Based Materials: From Blends and Composites to Gels and Complex Networks*, p. 1-6 (2013).
2. Nassar, M.A. and Y.R. Hassan, *Formulation and Application of Whey-Protein Based Coatings for Improved Paperboard Properties*. **56**, 213-224 (2013).
3. Niaounakis, M., *Biopolymers: Reuse, Recycling, and Disposal*. William Andrew (2013)
4. Joshi, J.R. and R.P. Patel, Role of biodegradable polymers in drug delivery. *Int J Curr Pharm Res*, **4**(4), 74-81 (2012).
5. Guo, J., et al., Design strategies and applications of citrate-based biodegradable elastomeric polymers, in natural and synthetic biomedical polymers. *Elsevier*. p. 259-285(2014).
6. Biswal, T., M. Priyadarsini, and S. Dash, *Sustainable bio-composite its manufacturing processes and applications*. *Egyptian Journal of Chemistry*, In Press (2018).
7. Adel, A.M., et al., Influence of Cellulose Polymorphism on Tunable Mechanical and Barrier Properties of Chitosan/Oxidized Nanocellulose Bio-Composites. *Egyptian Journal of Chemistry*, **60**(4), 639-652 (2017).

8. Mohamed, G., O. El-Shafey, and N.A. Fathy, Preparation of carbonaceous hydrochar adsorbents from cellulose and lignin derived from rice straw. *Egyptian Journal of Chemistry*, **60**(5), 793-804 (2017).
9. Beisl, S., A. Miltner, and A. Friedl, Lignin from micro-to nanosize: production methods. *International Journal of Molecular Sciences*, **18**(6), 1244 (2017).
10. Rangan, A., et al., *Lignin/Nanolignin and Their Biodegradable Composites*, in *Biodegradable Green Composites*. John Wiley & Sons, Inc Hoboken, NJ. p. 167-198 (2016).
11. Li, B., et al., *Drug-loaded polymeric nanoparticles for cancer stem cell targeting*. *Frontiers in Pharmacology*, **8**, 51 (2017).
12. De Jong, W.H. and P.J. Borm, Drug delivery and nanoparticles: applications and hazards. *International Journal of Nanomedicine*, **3**(2), 133 (2008).
13. Smith, C., *Nanoparticle Drug Delivery of Antitumor Agents* (2013).
14. Ghuttora, N., *Increase The Usage of Biopolymers and Biodegradable Polymers for Sustainable Environment* (2016).
15. Plamper, F.A., et al., Tuning the thermoresponsive properties of weak polyelectrolytes: aqueous solutions of star-shaped and linear poly (N, N-dimethylaminoethyl methacrylate). *Macromolecules*, **40** (23), 8361-8366 (2007).
16. Plamper, F.A., M. Ballauff, and A.H. Müller, Tuning the thermoresponsiveness of weak polyelectrolytes by pH and light: lower and upper critical-solution temperature of poly (N, N-dimethylaminoethyl methacrylate). *Journal of the American Chemical Society*, **129**(47), 14538-14539 (2007).
17. Plamper, F.A., et al., Star-shaped poly [2-(dimethylamino) ethyl methacrylate] and its derivatives: toward new properties and applications. *Polimery*, **59**(1), 66--73 (2014).
18. Gawish, S.M., S.E.-S. Mosleh, and A. Ramadan, Review Improvement of Polypropylene Properties by Irradiation/Grafting and Other Modifications. *Egyptian Journal of Chemistry*, **62**(1), 29-48 (2019).
19. Al-Snafi, A., The constituents and pharmacological properties of *Calotropis procera*-An Overview. *International Journal of Pharmacy Review & Research*, **5**(3), 259-275(2015).
20. Rahman, M. and C. Wilcock, A taxonomic revision of *Calotropis* (Asclepiadaceae). *Nordic Journal of Botany*, **11**(3), 301-308 (1991).
21. Grace, B., The biology of Australian weeds 45. *Calotropis procera* (Aiton) WT Aiton (2006).
22. Rahimi, M., Pharmacognostical aspects and pharmacological activities of *Calotropis procera*. *Bulletin of Environment, Pharmacology and Life Sciences*, **4**(2), 156-162 (2015).
23. Saeidnia, S., et al., Tryptophan and sterols from *Salvia limbata*. *Journal of Medicinal Plants*, **1**(37), 41-47 (2011).
24. Leaves, E., *International Journal of Pharmaceutical and Phytopharmacological Research (eIJPPR)*.
25. Saha, S., et al., Isolation and characterization of triterpenoids and fatty acid ester of triterpenoid from leaves of *Bauhinia variegata*. *Der Pharma Chemica*, **3**(4), 28-37 (2011).
26. Bulama, J., S. Dangoggo, and S. Mathias, Isolation and Characterization of Beta-Sitosterol from ethyl acetate extract of root bark of *Terminalia glaucescens*. *International Journal of Scientific and Research Publications* (2015).
27. da Rosa, M.P., et al., Extraction of organosolv lignin from rice husk under reflux conditions. *Biological and Chemical Research*, 87-98 (2017).
28. Gupta, A.K., S. Mohanty, and S. Nayak, Synthesis, characterization and application of lignin nanoparticles (LNPs). *Materials Focus*, **3**(6), 444-454 (2014).
29. Bhattacharya, S., et al., Antitumor efficacy and amelioration of oxidative stress by *Trichosanthes dioica* root against Ehrlich ascites carcinoma in mice. *Pharmaceutical Biology*, **49**(9), 927-935 (2011).
30. Sulaiman, G.M., M.S. Jabir, and A.H. Hameed, Nanoscale modification of chrysin for improved of therapeutic efficiency and cytotoxicity. *Artificial Cells, Nanomedicine, and Biotechnology*, 1-13 (2018).
31. Al-Shammari, A.M., et al., In vitro synergistic enhancement of Newcastle Disease Virus to 5-fluorouracil cytotoxicity against tumor cells.

- Biomedicines*, **4**(1), 3 (2016).
32. Zaki, M.Y., New approaches for the synthesis of thiophene derivatives with antitumor activities. Vol. 55. 549-560 (2012).
 33. Jabir, M.S., et al., Novel of nano delivery system for Linalool loaded on gold nanoparticles conjugated with CALNN peptide for application in drug uptake and induction of cell death on breast cancer cell line. *Materials Science and Engineering: C*, **94**, 949-964(2019).
 34. Tiwari, P., et al., Phytochemical screening and extraction: a review. *Internationale Pharmaceutica Scientia*, **1**(1), 98-106 (2011).
 35. Piombo, G., et al., Characterization of the seed oils from kiwi (*Actinidia chinensis*), passion fruit (*Passiflora edulis*) and guava (*Psidium guajava*). *Oléagineux, Corps Gras, Lipides*, **13**(2-3), 195-199 (2006).
 36. Siriwardhene, M., A. Abeyssekera, and A. Goonetilleke, Antihyperglycemic effect and phytochemical screening of aqueous extract of *Passiflora foetida* (Linn.) on normal Wistar rat model. *African Journal of Pharmacy and Pharmacology*, **27**(45), 2892-2894 (2013).
 37. Goldman, I. and R. Ortiz, A Life in Horticulture and Plant Breeding: The Extraordinary Contributions of Jules Janick. *Plant Breeding Reviews*, 291 (2018).
 38. Johnson, M., M. Maridass, and V. Irudayaraj, Preliminary phytochemical and anti-bacterial studies on *Passiflora edulis*. *Ethnobotanical Leaflets*, (1), 51 (2008).
 39. Saratha, V., S.I. Pillai, and S. Subramanian, Isolation and characterization of lupeol, a triterpenoid from *Calotropis gigantea* latex. *Int. J. Pharm. Sci. Rev. Res*, **10**(2), 54-57 (2011).
 40. Sammons, R.J., et al., Characterization of organosolv lignins using thermal and FT-IR spectroscopic analysis. *Bio Resources* **8** (2), 2752-2767, **8**(2), 2752-2767 (2013).
 41. Zielińska, D., D. Stawski, and A. Komisarczyk, Producing a poly (N, N-dimethylaminoethyl methacrylate) nonwoven by using the blowing out method. *Textile Research Journal*, **86**(17), 1837-1846 (2013).
 42. Sepe, M.P., *Thermal Analysis of Polymers*. Vol. 95. iSmithers Rapra Publishing (1997).
 43. Gopalakrishnan, S. and R. Sujatha, Comparative thermoanalytical studies of polyurethanes using Coats-Redfern, Broido and Horowitz-Metzger methods. *Der Chem Sin*, **2**(5), 103-117 (2011).
 44. El Khaldi-Hansen, B., M. Schulze, and B. Kamm, Qualitative and quantitative analysis of lignins from different sources and isolation methods for an application as a biobased chemical resource and polymeric material, in *Analytical Techniques and Methods for Biomass*. Springer. p. 15-44 (2016).
 45. Silva, F.A., F.H. Florenzano, and F.L. Pissetti, Synthesis and characterization of semi-interpenetrating polymer network based on poly (dimethylsiloxane) and poly [2-(dimethylamino) ethyl methacrylate]. *Journal of sol-gel science and technology*, **72**(2), 227-232 (2014).
 46. Khaghani, S., et al., Selective cytotoxicity and apoptogenic activity of Hibiscus sabdariffa aqueous extract against MCF-7 human breast cancer cell line. *Journal of Cancer Therapy*, **2**(03), 394 (2011).
 47. Katiyar, R., et al., VA-mycorrhizal association in arjuna and jamun trees in forest of Bhandara region, Maharashtra, India. *International Journal of Plant Sciences (Muzaffarnagar)*, **4**(1), 229-232 (2009).
 48. Sumithra, P., et al., *Pelagia Research Library*.
 49. Krajčovičová, Z., et al., Influence of Selected Triterpenoids On Chemoprevention And Therapy of Breast Cancer. *University Review*, **6**(1), (2012).
 50. MR Patlolla, J. and C. V Rao, Triterpenoids for cancer prevention and treatment: current status and future prospects. *Current Pharmaceutical Biotechnology*, **13**(1), 147-155 (2012).
 51. Nosrati, H., et al., Green and one-pot surface coating of iron oxide magnetic nanoparticles with natural amino acids and biocompatibility investigation. *Applied Organometallic Chemistry*, **32**(2), e4069 (2018).

دراسة السلوك الحراري والفعالية المضادة للسرطان لبعض الشبكات النانوية الجديدة المحضرة
للكنين والساندة للمركب التريبيني الثلاثي المعزول من اوراق نبات الديباج *Calotropis*
procera L

إيناس عبدالهادي زغير السويطي، باقر عبدالوهاب طاهر المياحي، عدنان جاسم محمد الفرطوسي
قسم الكيمياء – كلية العلوم – جامعة البصرة – البصرة - العراق.

الهدف من هذه الدراسة هو توفير مضاد حيوي لسرطان الثدي بواسطة مركب تريبيني ثلاثي معزول من نبات محلي رخيص ومتوفر (*Calotropis procera L.*) وتحضير شبكتين جديدتين متداخلتين من البوليمر (IPNs) بواسطة بوليمرات حيوية طبيعية مثل الكنين المحول للهيئة النانوية (lignin nanoparticles LNPs) وصناعية مثل البولي ميثا اكرلك اسد (MAA) و-2 داي ميثيل امينو اثيل ميثااكريليت (DMAEMA) كساندة للمركب المعزول. شخص المركب المعزول بواسطة تقنية الأشعة تحت الحمراء (IR) والرنين النووي المغناطيسي (1H-NMR) اما البوليمر المعزول والبوليمرات المحضرة فقد شخصت وقيمت بواسطة الأشعة تحت الحمراء، والتحليل الحراري (TGA) والمجهر الإلكتروني الماسح (SEM). تم اختبار فعالية كل من المركب التريبيني المعزول و LNPs و IPNs للمستخلص باستخدام MTT على خط الخلية MCF-7 لمدة 72 ساعة وبتراكيز مختلفة. وجدنا أن جميع النماذج أعطت تأثيراً مميئاً مختلفاً على الخلايا.